Slovak Journal of Civil Engineering

Vol. 33, 2025, No. 2, 36 – 45
DOI: 10.2478/sjce-2025-0010

INVESTIGATING THE PROBLEMS OF UNCONFINED NON-DARCY FLOWS THROUGH EMBANKMENT DAMS USING A DEPTH-AVERAGED MODEL

Yebegaeshet T. ZERIHUN[1*]

Abstract

Fully-developed turbulent flow-through coarse-grained porous media cannot be treated with the Dupuit approach based on Darcy's law unless Forchheimer's resistance equation is considered to account for non-linear effects arising from drag forces. By combining this equation with the Reynolds-averaged Navier-Stokes equations, a higher-order, depth-averaged model applicable to the flow of curvilinear seepage in a non-linear turbulent regime was developed. The governing equations were numerically solved with a hybrid scheme that adopts the finite-difference and finite-volume methods. The model's validity was then examined by carrying out numerical tests involving unconfined non-Darcy flows. The numerical results for such flows through rockfill structures with various geometric shapes were compared with the experimental data and produced a satisfactory agreement. The results of the study demonstrated that a depth-averaged model of this type is mostly preferred for accurately predicting the phreatic surface curvature and the exit height of the seepage line. Furthermore, the overall results confirmed the model's capability for adequately capturing the dynamic behavior of the turbulent seepage flow. The present model is therefore a useful tool for practicing engineers to evaluate the conceptual design of rockfill dams.

Address

[1] David & James – Engineering and Environmental Consultancy, 204 Albion Road, Victoria 3350, Australia

[*] ***Corresponding author:*** zyebegaeshet@gmail.com

Key words

- Non-Darcy flow,
- Non-linear resistance law,
- Rockfill dam,
- Turbulent seepage flow,
- Numerical simulation,
- Forchheimer's correction.

1 INTRODUCTION

A rockfill dam without an impervious core can be effectively used to reduce peak flood flows or to control the outflow from a detention basin. Unlike an earth dam, the quantity of water flowing through a rockfill dam is relatively large; hence, the need for a costly overflow structure can be obviated. Such a high velocity flow is known for a non-linear dependence of velocity on the hydraulic gradient and a deviation from Darcy's (1856) law (Slichter, 1899; Geertsma, 1974). In the vicinity of the downstream face of the dam, the phreatic surface is sharply curved so that the Dupuit (1863) approximation of the horizontal flow is invalid. Also, the line of seepage does not need to be tangent to the discharge face at the point of emergence. An accurate determination of the height of the exit point is practically significant, especially to analyze the stability of a proposed rockfill dam. A higher-order, depth-averaged model combined with Forchheimer's (1901) resistance equation is a valuable tool for a detailed study of the structure of the unconfined non-Darcy flow. It is worth mentioning that the problem investigated in this study deals with such a type of flow in a non-linear turbulent regime.

In the past, seepage flows in the non-linear regime have been experimentally studied. The experiments were carried out to fill in the knowledge gaps in the field of groundwater hydrodynamics, with a greater emphasis on the quantification of the resistance of a non-Darcy flow (e.g., Ergun, 1952; Wright, 1968; McCorquodale et al., 1978; van Gent, 1995a; Siddiqua et al., 2011; Shi et al., 2020). Recently, Ravindra et al. (2019) conducted experiments on flow-through rockfill dams without employing a permeameter test approach and overcame the size-scale limitation of the previous studies. For developing empirical equations describing the flow in a non-linear regime, these investigations aimed at exploring the salient features of the flow under a steady-state condition. Although the application of the resulting equations is limited by the scope of the experiments, the results of such investigations play a significant role in improving the performance of a numerical model.

Lower- and higher-order numerical models have been used to systematically study the non-Darcy flow. With the use of the assumption of a hydrostatic pressure distribution and a Forchheimer-type resistance in porous media, various investigators (Hansen et al., 1995; Bari and Hansen, 2002; Hosseini and Joy, 2007; Sarkhosh et al., 2020) presented one-dimensional (1D) models to simulate turbulent flow-through, coarse-grained porous media. Such a 1D approach oversimplifies the two-dimensional (2D) characteristics of the unconfined flow problem and substantially reduces the computational effort. As a consequence, it does not yield realistic solutions for the distribution of the pore pressure and the height of the exit point. As noted by Zerihun (2018, 2023a), the vertical velocity of the seepage flow cannot be overlooked in the analysis of this problem, especially in the vicinity of a free-outflow boundary. In this region, the flow patterns from the solutions of lower- and higher-order models are significantly different. To overcome the limitation of the lower-order approach, velocity and pressure correction coefficients for the effects of the phreatic surface curvature were applied by Hannoura (1978). As an alternative, 2D models under mesh-based or mesh-free approaches were also proposed for studying such a type of flow problem. Using a more general and rigorous approach, van Gent (1995b) developed a higher-order model based on the Navier–Stokes equations (Reynolds equations) to describe the unsteady turbulent flows in porous media. He applied the model to study the interaction between water waves and porous structures. By modifying the classical Navier–Stokes equations, Larese et al. (2015) proposed a numerical model for simulating the seepage flow inside a rockfill dam and an open-channel flow outside a porous structure. They examined the suitability of the numerical model using experimental data and obtained satisfactory results for the turbulent flow problems. A model that utilizes the finite-element discretization method was also developed and applied to investigate the non-Darcy flow problem (Sharif et al., 2001). Compared to a non-hydrostatic depth-averaged model, all these higher-order models require extra computational effort to solve large-scale problems. A smoothed particle hydrodynamics (SPH) method was recently used to simulate seepage flow through porous media (Holmes et al., 2011; Peng et al., 2017). For unsteady flow problems, it is challenging to treat the inflow and outflow boundaries using this approach (Ferrand et al., 2017). Such open boundaries involve a special treatment to handle Dirichlet and Neumann conditions. Besides, the accuracy, stability, and computational efficiency of the SPH method need further enhancement.

It is clear from the above discussion that although the breakdown of Darcy's law at high Reynolds numbers has been widely recognized, a higher-order treatment of unconfined seepage-flow problem involving turbulent flow has not been given adequate attention. To the author's knowledge, a higher-order, depth-averaged seepage-flow model has not been applied to investigate such a type of flow problem. In this study, the Reynolds-averaged Navier-Stokes (RANS) equations for seepage flow are combined with Forchheimer's resistance equation to develop a non-hydrostatic depth-averaged model that is applicable, within the limits of the validity of the resistance equation, to flow in a non-linear turbulent regime. In the Forchheimer equation, the non-Darcy pressure drop varies quadratically with the mass flux at higher values of the Reynolds numbers. Such a non-linear resistance equation was developed based on a sound rational basis (see, e.g., Irmay, 1958; Whitaker, 1996) and will be added to the RANS momentum equations as a dissipative term. As discussed by Chilton and Colburn (1931), the resistance to flow in granular material is made up of frictional resistance at the solid surfaces and energy losses due to successive expansions and contractions of pore spaces through which fluid is passing. For a non-Darcy flow, the latter is more dominant than the former one. The proposed model extends the treatment in the non-linear flow range by retaining relevant inertial terms in the RANS equations so that it can capture the realistic behavior of the 2D flow problems, which is strongly influenced by the effects of diverging and converging streamlines. Therefore, the study aims to apply this depth-averaged model to analyze non-Darcy flow problems and to determine if such a numerical model can adequately handle the non-linear effects. In addition, the impact of inaccurate characterization of the material properties of the porous media on the results of the model is examined. The model proposed here is of practical significance as it is applicable to several problems of unconfined flows through rockfill dams, rock drains, and banks. However, it is not suitable to analyze flows in non-homogeneous porous media built of layered systems with spatially varying porosities.

The remaining part of the work is organized as follows: in Section 2, a set of equations for modeling turbulent flow in porous media is developed, and the relevant methodology is discussed. Section 3 describes the development of a numerical scheme for the solutions of the equations. In Section 4, the reliability of the numerical model for steady and unsteady flow problems is tested against the experimental data. A short discussion about the expected significance of the proposed model is presented in Section 5. Finally, the main findings of the investigation are disclosed in Section 6.

2 GOVERNING EQUATIONS

The fundamental equations governing fluid flow, i.e., the RANS equations, are applicable to fluid flowing between the coarse grains of a porous media. These equations are adopted here but consider the porosity into both the continuity and momentum equations. The governing equations for turbulent flow through this media with a rectangular cross-section can be derived by depth averaging the following modified form of the RANS equations:

$$\frac{\partial}{\partial x}\left(\frac{u}{\lambda}\right)+\frac{\partial}{\partial z}\left(\frac{w}{\lambda}\right)=0, \tag{1}$$

$$\frac{\partial}{\partial t}\left(\frac{u}{\lambda}\right)+\frac{\partial}{\partial x}\left(\frac{u^2}{\lambda^2}\right)+\frac{\partial}{\partial z}\left(\frac{uw}{\lambda^2}\right)+\frac{1}{\rho}\frac{\partial p}{\partial x}=g\Gamma_1, \tag{2}$$

$$\frac{\partial}{\partial t}\left(\frac{w}{\lambda}\right)+\frac{\partial}{\partial x}\left(\frac{uw}{\lambda^2}\right)+\frac{\partial}{\partial z}\left(\frac{w^2}{\lambda^2}\right)+\frac{1}{\rho}\frac{\partial p}{\partial z}+g=g\Gamma_2, \tag{3}$$

where x and z are the horizontal and vertical coordinates, respectively; λ is the effective porosity of the porous media; u and w denote the bulk velocities in the horizontal and vertical directions, respectively; g is the gravitational acceleration; p is the pressure; ρ is the density of water; t is the time; and Γ_1 and Γ_2 are the coefficients of flow resistance due to viscous and turbulent frictions and inertial effects. The dynamic characteristics of the flow and the material properties of the porous media determine the relative significance of the components of the resistance. For flow-through coarse granular media, the turbulent and inertial components of the resistance are of greater importance (Gu and Wang, 1991). To account for such non-linear effects, the exponential and the Forchheimer resistance equations have been proposed in the past (Polubarinova-Kochina, 1962). It has been shown by several theoretical studies (Wright, 1968; Ahmed and Sunada, 1969; Tiss and Evans, 1989; Joy, 1991; Ma and Ruth, 1993) that Forchheimer's equation can describe the physical process for a considerable range of Reynolds numbers more accurately than the exponential equation. Therefore, a Forchheimer-type equation is employed here for accurately predicting Γ_1 and Γ_2. The use of such an equation is necessary due to the significance of the convective inertial effects at higher Reynolds numbers. It should be emphasized that this study is restricted to seepage flow in a homogeneous and isotropic porous media.

To simplify the complex flow phenomena, the variations of the flow variables in the lateral direction and the effects of the capillary fringe are ignored. For the turbulent flow problem considered, the latter approximation does not introduce significant errors. Assuming that it is constant over the vertical, the horizontal velocity can be expressed as

$$u_e=\frac{u}{\lambda}=\frac{q}{\lambda H}, \tag{4}$$

where q is the seepage discharge per unit width; and u_e is the pore velocity in the horizontal direction. After substituting Equation (4) into Equation (1), the resulting expression is integrated from the bedrock to an arbitrary point. Using the kinematic boundary condition at the bedrock in the final result, the equation of the vertical velocity is obtained as follows:

$$w_e=\frac{w}{\lambda}=\frac{\partial H}{\partial t}\Lambda-\frac{q}{\lambda H}\frac{\partial H}{\partial x}(1-\Lambda)+\frac{q}{\lambda H}\frac{\partial \eta}{\partial x}, \tag{5a}$$

$$\Lambda=\frac{z-Z}{\eta-Z}, \tag{5b}$$

where w_e is the pore velocity of the seepage flow in the vertical direction; Λ is a non-dimensional vertical coordinate; H is the flow depth; z is the vertical coordinate of a point in the flow field; Z is the bedrock elevation; and η is the phreatic surface elevation (defined in Fig. 1). The vertical profile of the pressure distribution can be described by the following equation:

$$p=(\rho g H+p_D)(1-\Lambda), \tag{6}$$

where p is the total pressure; and p_D is the dynamic pressure at the bedrock.

Using Equations (4), (5a), and (6), the continuity equation and the RANS momentum equations are integrated over the depth in order to express the hydraulic characteristics of the turbulent seepage flow by the flow depth and discharge. After applying the kinematic and dynamic boundary conditions, the following depth-averaged equations for an accretion-free flow are obtained:

$$\frac{\partial H}{\partial t}+\frac{\partial}{\partial x}\left(\frac{q}{\lambda}\right)=0, \tag{7}$$

$$\begin{aligned}&\frac{\partial}{\partial t}\left(\frac{q}{\lambda}\right)+\frac{\partial}{\partial x}\left(\frac{q^2}{\lambda^2 H}+\frac{gH^2}{2}\right)\\&+\left(gH+\frac{p_D}{\rho}\right)\frac{\partial Z}{\partial x}+\frac{\partial}{\partial x}\left(\frac{Hp_D}{2\rho}\right)-gH\bar{\Gamma}_1=0,\end{aligned} \tag{8}$$

$$\begin{aligned}&\frac{\partial}{\partial t}\left(\frac{q}{2\lambda}\left(\frac{\partial H}{\partial x}+2\frac{\partial Z}{\partial x}\right)\right)+\frac{\partial}{\partial x}\left(\frac{q^2}{2\lambda^2 H}\left(\frac{\partial H}{\partial x}+2\frac{\partial Z}{\partial x}\right)\right)\\&-\frac{\partial}{\partial t}\left(\frac{Hq_x}{2\lambda}\right)-\frac{\partial}{\partial x}\left(\frac{qq_x}{2\lambda^2}\right)-\frac{p_D}{\rho}-gH\bar{\Gamma}_2=0,\end{aligned} \tag{9}$$

where q_x is the seepage discharge per unit length per unit width; and the overbar denotes a depth-averaged parameter. From Equation (6), the expression for the piezometric head H_p is obtained as

$$H_P=\left(\eta+\frac{p_D}{\gamma}\right)(1-\Lambda)+\eta\Lambda, \tag{10}$$

where γ is the unit weight of the fluid. For non-Darcy flows through coarse-grained porous media, the resistance due to form drag dominates the bed friction. Hence, the flow resistance parameters are reckoned from the extended form of Forchheimer's equation (Irmay, 1958) as follows:

$$\bar{\Gamma}_1\cong-\mu_1\bar{U}-\mu_2\bar{U}\left(\bar{U}^2+\bar{w}^2\right)^{1/2}-\frac{\mu_3}{gH}\frac{\partial}{\partial t}\left(\frac{q}{\lambda}\right), \tag{11a}$$

$$\bar{\Gamma}_2\cong-\mu_1\bar{w}-\mu_2\bar{w}\left(\bar{U}^2+\bar{w}^2\right)^{1/2}-\frac{\mu_3}{gH}\frac{\partial}{\partial t}\left(\frac{q}{2\lambda}\left(\frac{\partial H}{\partial x}+2\frac{\partial Z}{\partial x}\right)\right), \tag{11b}$$

$$\bar{w}=\frac{q}{2\lambda H}\left(\frac{\partial H}{\partial x}+2\frac{\partial Z}{\partial x}\right)+\frac{1}{2}\frac{\partial H}{\partial t}, \tag{11c}$$

$$\mu_3=\left(\frac{1-\lambda}{\lambda}\right)C_m, \tag{11d}$$

where $\bar{U}$ ($=u_e$) is the depth-averaged horizontal velocity; C_m is the virtual mass coefficient; μ_1 and μ_2 are dimensional constants determined by the properties of the fluid and porous media; and μ_3 is an inertial correction coefficient that accounts for the additional hydraulic resistance generated by the virtual mass of discrete grains within the porous matrix (Sollitt and Cross, 1972; Hannoura and McCorquodale, 1978). Such a local acceleration effect becomes more significant for unsteady flows through coarse granular media. The values of these coefficients slowly vary with the Reynolds numbers; they can be estimated by empirical equations (see Kozeny, 1927; Ergun, 1952; Gu and Wang, 1991). The unsteady terms appearing in Equations (11a) and (11b) are relatively insignificant for a quasi-steady flow situation (Irmay, 1958). By ignoring the non-linear effects at very low Reynolds numbers, a flow model obeying Darcy's law can be recovered from the above equations. For flow outside porous media ($\lambda = 1$), the resistance terms are replaced by the corresponding equations for an open-channel flow. Such a curvilinear flow model provides data at the open boundary sections for the application of the proposed turbulent seepage-flow model.

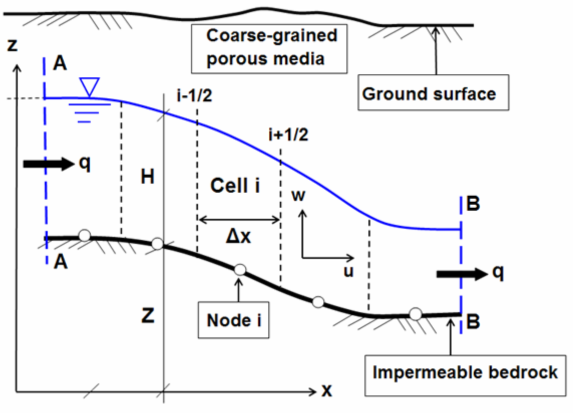

Fig. 1 *Schematic representation of unconfined seepage flows through coarse-grained porous media. The inflow and outflow sections are indicated by A-A and B-B, respectively*

3 NUMERICAL SCHEME

The governing equations are partial differential equations and, as such, are amenable to solution by a suitable numerical scheme. In this study, the finite-difference, finite-volume, and the forward Euler time-stepping methods were used to discretize these equations. The salient attributes of the numerical scheme, such as the procedure for flux computation, the time-stepping method, and the implicit numerical technique, will only be briefly summarized here; further details regarding the numerical model can be found in Zerihun (2024). To obtain a numerical solution to these non-linear equations using the proposed scheme, it is necessary to delineate a computational domain and to specify the relevant initial and boundary conditions.

3.1 Time Stepping and Numerical Flux Computation

The preceding equations for a 2D non-Darcy flow may be written in a vector form as

$$\frac{\partial U}{\partial t}+\frac{\partial F(U)}{\partial x}=S, \tag{12}$$

where the unknown conserved variables U, the fluxes $F(U)$, and the source terms S are given by

$$U=\begin{pmatrix} H \\ \left(\dfrac{1+\mu_3}{\lambda}\right)q \\ \left(\dfrac{1+\mu_3}{2\lambda}\right)\left(\dfrac{\partial H}{\partial x}+2\dfrac{\partial Z}{\partial x}\right)q \end{pmatrix}, \tag{13a}$$

$$F(U)=\begin{pmatrix} \dfrac{q}{\lambda} \\ \dfrac{q^2}{\lambda^2 H}+\dfrac{gH^2}{2} \\ \dfrac{q^2}{2\lambda^2 H}\left(\dfrac{\partial H}{\partial x}+2\dfrac{\partial Z}{\partial x}\right) \end{pmatrix}, \tag{13b}$$

$$S=\begin{pmatrix} 0 \\ -\left(gH+\dfrac{p_D}{\rho}\right)\dfrac{\partial Z}{\partial x}-\dfrac{\partial}{\partial x}\left(\dfrac{Hp_D}{2\rho}\right)+g\Psi_1 \\ \dfrac{p_D}{\rho}+g\Psi_2+\Psi_3 \end{pmatrix}, \tag{13c}$$

$$\Psi_1=-\mu_1 H\overline{U}-\mu_2 H\overline{U}\left(\overline{U}^2+\overline{w}^2\right)^{1/2}, \tag{13d}$$

$$\Psi_2=-\mu_1 H\overline{w}-\mu_2 H\overline{w}\left(\overline{U}^2+\overline{w}^2\right)^{1/2}, \tag{13e}$$

$$\Psi_3=\frac{\partial}{\partial t}\left(\frac{Hq_x}{2\lambda}\right)+\frac{\partial}{\partial x}\left(\frac{qq_x}{2\lambda^2}\right) \tag{13f}$$

Discretizing the integral form of Equation (12) using the finite-volume method (Hirsch, 2007) and applying the Euler time-stepping scheme to the resulting expression yields the following equation for a space-time grid:

$$U_i^{N+1}=U_i^N-\frac{\Delta t}{\Delta x}\left(F(U)_{i+1/2}^N-F(U)_{i-1/2}^N\right)+\Delta t S_i^N, \tag{14}$$

where Δx is the step size in the streamwise x -direction; i is a computational point or cell index; and Δt is the time step. In the above equation, the superscript N refers to the variables at the current time level, while $F(U)_{i\pm 1/2}$ are the numerical fluxes at the left and right faces of cell i. Equation (14) is numerically solved by applying both explicit and implicit methods.

To apply the finite-volume method, the values of the variables on the cell interfaces need to be reconstructed using their respective cell-averaged values. Since a homogeneous porous media is considered here, the total variation-diminishing version of a fourth-order monotone upstream-centered scheme for the conservation laws (MUSCL-TVD), which was introduced by Yamamoto and Daiguji (1993), is applied to reconstruct the variables. The MUSCL-TVD scheme utilizes two-step limiter functions to avoid spurious oscillations and to maintain monotonicity near any shocks. Additionally, the weighted surface-depth gradient method (Aureli et al., 2008) is employed to evaluate the flow depth at the cell interfaces. This method can prevent the prevalence of numerical oscillations arising from a discontinuous bedrock profile or steep bedrock gradient and is useful for obtaining a well-balanced numerical scheme. Based on the reconstructed interface values, the numerical fluxes are reckoned by the Harten-Lax-van Leer (HLL) approximate Riemann solver (Harten et al., 1983) on a space-time grid.

3.2 Solution Method

Because of its simple structure, the equation of continuity is solved explicitly at all the time levels. However, an implicit method is employed to solve Equations (8) and (9) for the unknown conserved variables q and p_D at each time step. Such a method has been proved to be numerically accurate and stable (see Soares-Frazão and Guinot, 2008; Zerihun, 2024). Using Equation (14) and the finite-difference approximations (Bickley, 1941) for the various derivatives appearing in the source terms, these momentum equations are discretized. The fluxes and source terms in the resulting equations are reckoned using the known values of the variables from the preceding time levels, giving a system of non-linear equations. These implicit sets of algebraic equations are first reduced to a linear form by the Newton–Raphson method and then solved with the lower-upper (LU) decomposition method, as was previously applied by Zerihun (2018, 2020a). As a solution to the problem of the unconfined turbulent flow, cell-averaged values of the conserved variables at different time levels are obtained from the numerical scheme.

4 RESULTS OF THE VALIDATION OF THE MODEL

The applicability of the numerical model was investigated by analyzing non-Darcy, steady and unsteady flow problems with various Froude numbers ($0.03 \leq F \leq 0.32$), where F is the Froude number). It is obvious from the characteristics of the test problems that a supercritical seepage flow ($F > 1$) rarely occurs in coarse-grained porous media. The three seepage-flow problems considered here are: (i) an unsteady flow through a rectangular-shaped dam; (ii) a steady flow through a trapezoidal-shaped dam; and (iii) a dam-break flow through a rockfill structure. The test case of a steady flow was iteratively solved as a quasi-steady flow problem by treating the time as an iteration parameter until an asymptotic final solution was attained. For the first two test cases, the initial condition of the flow was presumed to be a subcritical uniform flow ($p_D = 0$) with the specified values of the flow depth and discharge at the inflow section. For the test case of the dam-break wave, an initial condition similar to the first set-up of the experiment was imposed. It is also assumed that the mean flow characteristics immediately outside and inside the porous media represent the same flow situation, which is free of jets and wakes. Such an approximate treatment does not substantially affect the quality of the numerical results. For all the cases, the height of the exit point is determined from the interior cell values using an extrapolation equation (Press et al., 2007).

For minimizing the numerical error arising from the effects of the spatial discretization, a step size smaller than 3.5% of the flow depth at the inflow section was employed. In addition to this, a numerical stability criterion based on the modified Courant–Friedrichs–Lewy equation (van Gent et al., 1994) was applied to limit the computational time step. Accordingly, a time step of less than 0.15 s was applied to achieve stable and accurate solutions.

4.1 Turbulent Flow through a Rectangular-Shaped Dam

Hosseini and Joy (2007) performed a series of experiments to investigate non-Darcy flows through a homogeneous dam with a rectangular section. The test results of an embankment dam made of rockfill material with a median grain size of 8.7 mm (Test SU4) were selected to corroborate the numerical results. The experiments were conducted in a flume having a width of 603 mm and a bed slope of 0.58%. The embankment was 1.50 m long, with a height of 400 mm; and the upstream and downstream faces were made vertical by a rigid screen covered with a wire mesh. The porosity of the media was found to be 0.48. A sharp-crested triangular (V-notch) weir installed upstream of the dam was used to measure the inflow discharge. Additionally, pressure transducers were used to record the flow depths in an unsteady flow condition. For more details about the experimental system, see Hosseini and Joy (2007).

For this unsteady flow problem, the experimentally determined flow depth and discharge hydrographs (as illustrated in Fig. 2) were specified as inflow boundary conditions at a section immediately downstream of the V-notch weir. The open-channel flow version of the current model (for $\lambda = 1$) was applied between this section and the upstream face of the rockfill dam. The experimental phreatic surface profiles for this flow situation are shown in Fig. 3, together with the numerical results. In this figure, the bottom length of the dam L was used as a characteristic parameter to normalize the phreatic surface elevation and the horizontal distance in the streamwise direction. As can be seen from Fig. 3, the depth-averaged model reasonably mimicked the profiles of the phreatic surface at various time levels, with the mean absolute relative error (MARE) values of less than 3%. At the earlier computational time ($t = 26$ s), the unconfined seepage flow was highly transient, and its phreatic surface elevation was slightly underestimated by the model. At a later simulation time, the simulated phreatic surface profiles closely matched the experimental results. For this transient, quasi-hydrostatic seepage flow, the effects of the flow resistance due to form drag on the non-Darcy pressure drop were significant. As demonstrated by its results, the proposed model effectively handled these effects.

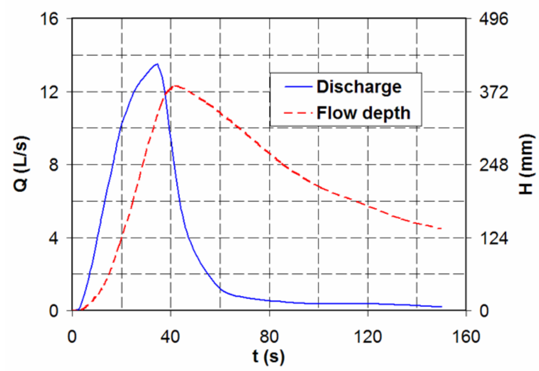

Fig. 2 *Input hydrographs for an unsteady seepage-flow problem. The seepage discharge is denoted by Q*

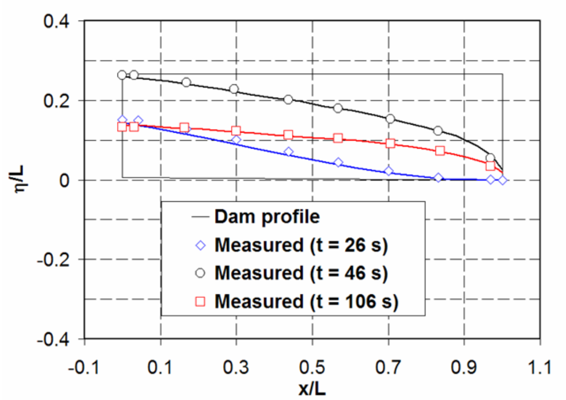

Fig. 3 *Comparison of computed phreatic surface profiles with the data of Test SU4. The solid lines with the colors of the matching experimental data indicate the numerical results*

4.2 Turbulent Flow through a Trapezoidal-Shaped Dam

The applicability of the model was further examined with the measurements of the elevation of the phreatic surface for steady flows through trapezoidal-shaped dams (Hansen, 1992). The selected experiments were carried out in a glass-walled flume with a width of 385 mm using three dam configurations. The homogeneous dams had a constant upstream-face slope (θ) of 45º, and their downstream faces sloped at 18.43, 26.57, and 45º. They were made of rockfill material with a median grain size of 25 mm and had a height of 500 mm. The porosity of the material used in the experiments was 0.44. The streamwise variations of the elevations of the phreatic surface were measured under a steady-state condition. For further information regarding the experimental system, see Hansen (1992).

As mentioned before, this steady flow problem was solved by applying a quasi-steady flow approach. In this approach, the experimental flow depths and discharges at the inflow section were defined by a step function and specified as boundary conditions at this section. Typical input hydrographs of the test case are shown in Fig. 4. Fig. 5 displays the streamwise variations of the elevation of the phreatic surface for various discharges. The results of the model were in good agreement with the experimental data. The MARE values of the computed results varied between 2.9 and 6.5%. The flow depth at the point of the first flow's emergence (height of the exit point) and the phreatic surface curvature were accurately predicted, regardless of the steepness of the downstream-face slope β. The results of the test attested that the proposed model is capable of accurately mimicking the flow pattern near the point of emergence, where the effects of the vertical velocity are significant. This signifies that a higher-order, depth-averaged model must be used for accurate predictions of the local flow characteristics of such a type of turbulent seepage flow.

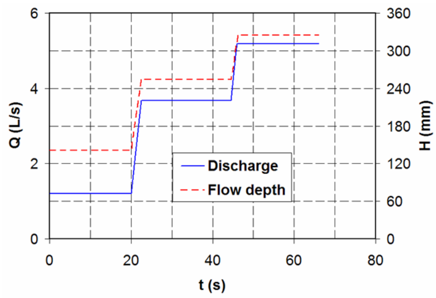

Fig. 4 *Input hydrographs for the quasi-steady flow approach (Test GF29d)*

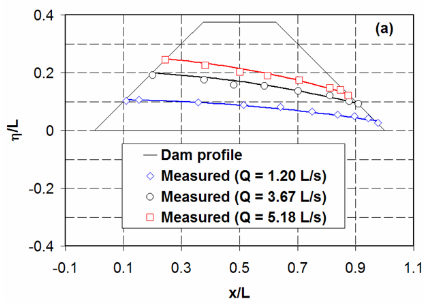

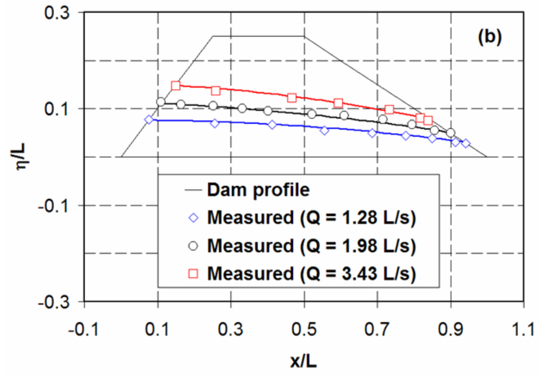

Fig. 5 *Comparison of computed phreatic surface profiles with the experimental data: (a) Test GF29d (θ = β = 45º); and (b) Test GF31c (θ = 45º and β = 26.57 º). The solid lines with the colors of the matching experimental data indicate the numerical results*

4.3 Dam-Break Flow through a Rockfill Structure

The model's reliability was thoroughly assessed by modeling the complex seepage flows due to a sudden removal of the gate of the reservoir. The data of one of Lin's (1998) experiments were chosen to verify the results. He conducted the experiments in a water tank that was 892 mm long, 440 mm wide, and 580 mm deep. A rectangular-shaped rockfill structure with a length of 290 mm and a height of 370 mm was placed in the middle of the tank. This homogeneous structure was constructed using crushed rock with a median grain size of 15.9 mm and a porosity of 0.49. A vertical gate, which was installed 20 mm away from the upstream face of the porous structure, was used to generate the flood wave. The initial water depths in the sections upstream and downstream of the vertical gate were 250 and 25 mm, respectively. At the beginning of the experiment, the gate was manually opened (duration of about 0.1 s). The phreatic surface profiles at various times were filmed by a normal CCD camera with a frame rate of 10 fps.

For this problem, a zero-flux boundary condition ($q(t) = 0$) and experimentally determined flow depths were specified at the upstream dead-end section. Similar to the previous unsteady flow test case, part of the flow between this section and the upstream face of the porous structure was modeled by an open-channel flow model. Fig. 6 compares the computed results for the phreatic surface profile with the experimental data during the period of the transient phenomenon. As depicted in the figure, the proposed model accurately reproduced the phreatic surface profiles for $t \geq 1$ s, with the MARE values of less than 2%. In the vicinity of the center of the porous structure ($0.32 < x/L < 0.65$), however, the model underestimated the level of the phreatic surface at the earlier stage ($t = 0.2$ s). This deviation might be the consequence of slowly lifting the vertical gate during the experiments, which triggered an earlier movement of the lower part of the water front. As expected, such an unsteady wave was damped out quickly by the extreme roughness of the coarse rock. For this test case, the overall quality of the computed results is satisfactory, demonstrating the model's capacity for handling the non-linear effects.

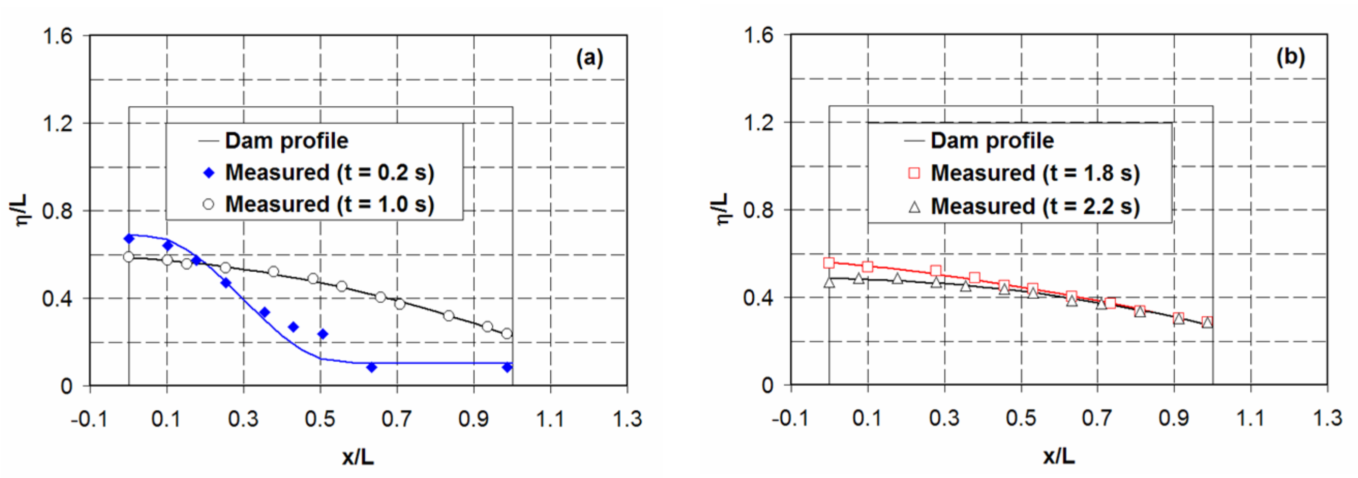

Fig. 6 *Temporal variation in phreatic surface elevations for non-Darcy flow through a rockfill structure. The solid lines with the colors of the matching experimental data of Lin (1998) indicate the numerical results*

4.4 Effects of the Rockfill Material Parameters

To examine the effect of the properties of the rockfill material on the results of the model, a sensitivity analysis was performed for selected parameters. The porosity λ and the median grain size of the rockfill material φ were considered and varied one at a time during the analysis. The roughness characteristics of the non-Darcy flow are strongly affected by the magnitudes of these parameters. The hypothetical values above and below the experimentally determined values of the parameters were used to examine their effects on the results. Boundary conditions similar to the previous steady flow test case were imposed at the inflow section. Fig. 7 compares the results of the analysis with the experimental data of Hansen (1992). For the given discharges with lower values of porosity and material grain size, the model overestimates the phreatic surface elevations. This is due to the fact that decreasing the values of these parameters increases the contributions of the viscous and turbulent components of the resistance. As a result, a higher pressure drop is needed to pass the fluid through the pore spaces. The converse is true in the case of higher values of these parameters. For these large values, the effects of the local turbulence and inertia become more predominant. It can be inferred from this investigation that the hydraulic characteristics of the unconfined seepage flow are significantly influenced by the material properties. In general, the results of the analysis demonstrated that the numerical solutions are highly sensitive to the porosity and the grain size of the rockfill material. Hence, an accurate characterization of the material properties is vital for the proper predictions of the mean flow characteristics of non-Darcy flows. The results also suggest that approximating the spatially-varied material properties by the mean values significantly affects the accuracy of the proposed model. The model has to be generalized to include the effects of such variations on the behavior of the turbulent seepage flow, which are common in non-homogeneous and anisotropic porous media.

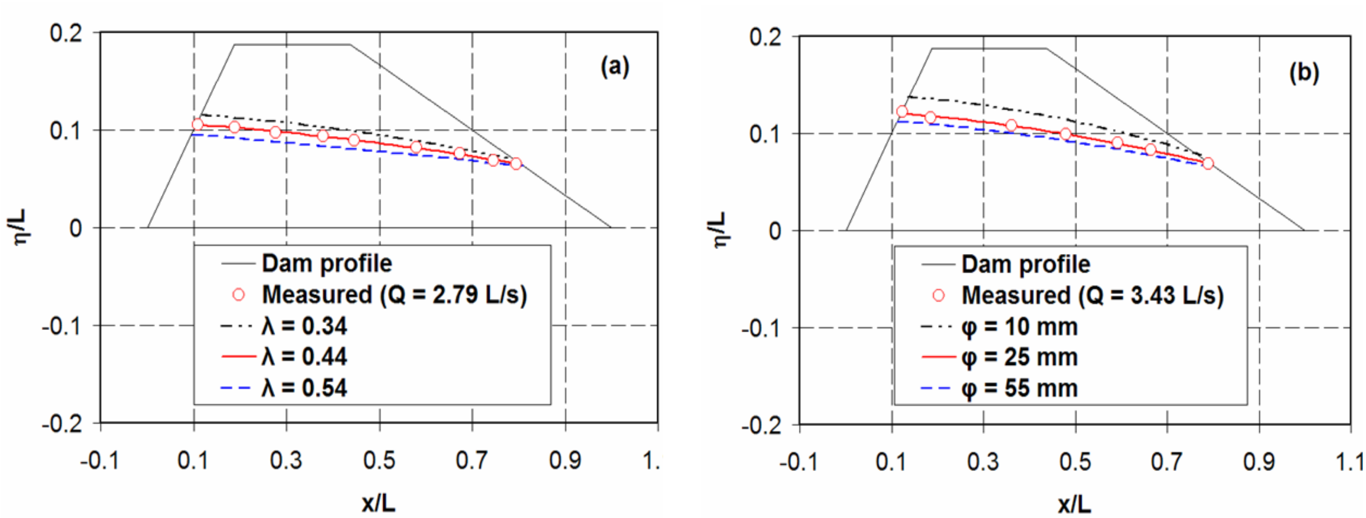

Fig. 7 *Phreatic surface profiles for various values of porosity λ and grain size of the rockfill material φ. The data of Test GF34a ($\theta = 45^o$ and $\beta = 18.43^o$) from the Hansen (1992) experiments were used to verify the numerical results*

5 DISCUSSION

The results of the preceding numerical investigation revealed that the dynamic characteristics of the turbulent seepage flow were satisfactorily simulated by the proposed non-hydrostatic seepage-flow model. This relatively simple and computationally efficient numerical model can provide a great deal of information about the pattern of the flow, including streamwise variations of the flow depth, seepage discharge, and piezometric head. In engineering practice, such information can be utilized to improve a preliminary design of a homogeneous rockfill dam. For instance, the height of the exit point and the grain sizes of the dam material are relevant to assess the potential of unraveling failure. Furthermore, the consequences of changes in the design variables can be more easily and quickly studied by simulating scenarios using the proposed model. In the case of the design of a rockfill dam with a central core (a zoned rockfill dam), the preliminary analysis at the initial design stage can be done by ignoring the effects of the thin, impervious core element. The results of this simplified approach can be refined at the final design stage by using a three-dimensional high-resolution model. This modeling technique has the ability to handle long-runs and deal with large-scale problems, thereby saving computational time and cost.

For a reservoir routing problem, the model can adequately predict the outflow discharge hydrograph for flow through a rockfill type of detention dam. Similar to the overflow discharge of an embankment weir (see Zerihun, 2020b, 2023b), its results can be further analyzed to develop a stage-discharge curve under a steady-flow situation, thereby simplifying the routing procedure. For a spatially-varied flow model (Zerihun, 2019), such a rating curve can provide the required lateral inflow data to effectively simulate an open-channel flow with a spatially-increasing discharge along the seepage face of a trapezoidal rockfill dam.

It should be noted that due to scarcity of field data, the model was validated using laboratory-scale experimental data. An assessment of the model's performance based on field data is needed to enhance its reliability.

6 CONCLUSIONS

In this study, the Reynolds-averaged Navier-Stokes equations for seepage flow were combined with Forchheimer's (1901) resistance equation to obtain a higher-order, depth-averaged model applicable to flows in non-linear turbulent regimes. The proposed model obviated the drawbacks of the previous one-dimensional models, which ignored the effects of the phreatic surface curvature (e.g., Hansen et al., 1995; Hosseini and Joy, 2007; Sarkhosh et al., 2020). These non-linear equations were numerically solved with a hybrid scheme that implements the finite-difference and finite-volume methods. The model's applicability was then examined by carrying out numerical tests involving unconfined non-Darcy flows through coarse-grained porous media. The results obtained for the phreatic surface profile of such flows through homogeneous rockfill structures with various geometries were verified using experimental data under steady and unsteady flow conditions.

For the test of an unsteady flow through a rockfill dam with a rectangular section, the numerical model reasonably mimicked the profiles of the phreatic surface at various time levels, with the mean absolute relative errors of less than 3%. Likewise, the results of a comparison of the computed and measured results for the case of steady flows through trapezoidal dams confirmed the model's capability for accurately describing the dynamic characteristics of the turbulent seepage flow. For this test, the predictions showed a close agreement with the experiments. In addition, the depth of the flow at the point of the first flow's emergence and the phreatic surface curvature were accurately predicted, regardless of the steepness of the slope of the downstream face. In both cases, the effects of the flow resistance due to the form drag on the non-Darcy pressure drop are significant. The proposed model effectively handled these effects.

Finally, the model's performance was further investigated by considering the dam-break flow through a rockfill structure. The model accurately reproduced the phreatic surface profiles for $t \geq 1$ s, with the mean absolute relative errors of less than 2%. However, the quality of its results was not satisfactory in the flow zone close to the center of the porous structure ($0.32 < x/L < 0.65$) at a computational time of 0.2 s. This deviation may be attributed to an experimental error associated with the lifting of the vertical gate. It is concluded from this study that the results of the model for the phreatic surface profile and piezometric head can be used to evaluate the stability of rockfill dams and to improve the preliminary design of these structures. The proposed model will be extended by coupling its equations with an advection-dispersion module to address water quality issues in buried streams due to the disposal of mine waste.

REFERENCES

AHMED, N. and D. K. SUNADA (1969). *Non-linear flow in porous media. J. Hydraul.* Div., 95(HY6), 1847–1858.

AURELI, F., A. MARANZONI, P. MIGNOSA and C. ZIVERI (2008). *A weighted surface-depth gradient method for the numerical integration of the 2D shallow-water equations with topography.* Adv. Water Resour., 31(7), 962–974.

BARI, R. and D. HANSEN (2002). *Application of gradually-varied flow algorithms to simulate buried streams.* J. Hydraul. Res., 40(6), 673–683.

BICKLEY, W. G. (1941). *Formulae for numerical differentiation.* Math. Gaz., 25(263), 19–27.

CHILTON, T. H. and A. P. COLBURN (1931). *Pressure drop in packed tubes.* Ind. Eng. Chem. Res., 23(8), doi:10.1021/ie50260a016. 913-919.

DARCY, H. (1856). *Les Fontaines Publiques de la Ville de Dijon: Exposition et Application des Principes à Suivre et des Formules à Employer dans les Questions de Distribution d'Eau (The Public Fountains of the City of Dijon: Exposition and Application of the Principles to be Followed and the Formulas to be Used in Questions of Water Distribution).* Dalmont: Paris, France, 590–594 [in French].

DUPUIT, J. (1863). *Études Théoriques et Pratiques sur le Mouvement des Eaux dans les Canaux Découverts et a Travers les Terrains Perméables (Theoretical and Practical Studies on Water Movement in Open Channels and across Permeable Terrains).* deuxième édition; Dunod: Paris, France, 229–293 [in French].

ERGUN, S. (1952). *Fluid flow through packed columns.* Chem. Engrg. Progress, 48(2), 89–94.

FERRAND, M., et al. (2017). *Unsteady open boundaries for SPH using semi-analytical conditions and Riemann solver in 2D.* Comput. Phys. Commun., 210, 29–44.

FORCHHEIMER, P. (1901). *Wasserbewegung durch boden (Water movement through soil).* Zeits. V. deutsch. Ing., 45, 1782–1788 [in German].

GEERTSMA, J. (1974). *Estimating the coefficient of inertial resistance in fluid flow through porous media.* Soc. Pet. Eng. J., 14(5), 445–450.

GU, Z. and H. WANG (1991). *Gravity waves over porous bottoms.* Coast. Eng., 15(5-6), 497–524.

HANNOURA, A. A. (1978). *Numerical and Experimental Modeling of Unsteady Flow in Rockfill Embankments.* Ph.D. Thesis, University of Windsor, Windsor, ON, Canada.

HANNOURA, A. A. and J. A. MCCORQUODALE (1978). *Virtual mass of coarse granular media*. J. Waterw. Port Coast. Ocean Div., 104(WW2), 191–200.

HANSEN, D. (1992). *The Behavior of Flow through Rockfill Dams.* Ph.D. Thesis, University of Ottawa, Ottawa, ON, Canada.

HANSEN, D., V. K. GARGA and D. R. TOWNSEND (1995). *Selection and application of a one-dimensional non-Darcy flow equation for two-dimensional flow through rockfill embankments.* Can. Geotech. J., 32(2), 223–232.

HARTEN, A., P. D. LAX and B. van LEER (1983). *On upstream differencing and Godunov-type scheme for hyperbolic conservation laws.* SIAM Rev. Soc. Ind. Appl. Math., 25(1), 35–61.

HIRSCH, C. (2007). *Numerical Computation of Internal and External Flows: Vol. 1 Fundamentals of Computational Fluid Dynamics.* 2nd ed., Elsevier: Oxford, UK, 208–209.

HOLMES, D. W., J. R. WILLIAMS and P. TILKE (2011). *Smooth particle hydrodynamics simulations of low Reynolds number flows through porous media.* Int. J. Numer. Anal. Methods Geomech., 35(4), 419–437.

HOSSEINI, S. M. and D. M. JOY (2007). *Development of an unsteady model for flow through coarse heterogeneous porous media applicable to valley fills.* Int. J. River Basin Manag., 5(4), 253–265.

IRMAY, S. (1958). *On the theoretical derivation of Darcy and Forchheimer formulas.* Trans. AGU, 39(4), 702–707.

JOY, D. M. (1991). *Non-linear flow in a coarse porous media.* In: Proceedings of the 10th Canadian Hydrotechnical Conference, CSCE, Vancouver, BC, Canada, 29–31 May, 1, 106–115.

KOZENY, J. (1927). *Über kapillare leitung des wassers im boden (Via capillary conduction of water in the soil).* Sitzungsber. Akad. Wiss. Vienna, 136, 271–306 [in German].

LARESE, A., R. ROSSI and E. OÑATE (2015). *Finite-element modeling of free-surface flow in variable porosity media.* Arch. Computat. Methods Eng., 22(4), 637–653.

LIN, P. (1998). *Numerical Modeling of Breaking Waves.* Ph.D. Thesis, Cornell University, Ithaca, NY, USA.

MA, H. and D. W. RUTH (1993). *The microscopic analysis of high Forchheimer number flow in porous media.* Transp. Porous Media, 13, 139–160.

MCCORQUODALE, J. A., A. A. HANNOURA and M. SAM NASSER (1978). *Hydraulic conductivity of rockfill. J. Hydraul.* Res., 16(2), 123–137.

PENG, C., G. XU, W. WU, H. S. YU and C. WANG (2017). *Multiphase SPH modeling of free-surface flow in porous media with variable porosity.* Comput. Geotech., 81, 239–248.

POLUBARINOVA-KOCHINA, P. Ya. (1962). *Theory of Groundwater Movement.* Princeton University Press: Princeton, NJ, USA, 25–26.

PRESS, W. H., S. A. TEUKOLSKY, W. T. VETTERLING and B. P. FLANNERY (2007). *Numerical Recipes in C++*. 3rd ed., Cambridge University Press: Cambridge, UK, 118–119.

RAVINDRA, G. H. R., F. G. SIGTRYGGSDÓTTIR and Ø. A. HØYDAL (2019). *Non-linear flow through rockfill embankments.* J. Appl. Water Eng. Res., 7(4), 247–262.

SARKHOSH, P., A. SALAMA and Y.-C. JIN (2020). *A one-dimensional semi-implicit finite volume modeling of non-inertia wave through rockfill dams.* J. Hydroinform., 22(6), 1485–1505.

SHARIF, N. H., N.-E. WIBERG and M. LEVENSTAM (2001). *Free-surface flow through rockfill dams analyzed by FEM with level set approach.* Comput. Mech., 27, 233–243.

SHI, W., T. YANG and S. YU (2020). *Experimental investigation on non-Darcy flow behavior of granular limestone with different porosity.* J. Hydrol. Eng., 25(8), doi:10.1061/(ASCE)HE.1943-5584.0001966.

SIDDIQUA, S., J. A. BLATZ and N. C. PRIVAT (2011). *Evaluating turbulent flow in large rockfill. J. Hydraul.* Eng., 137(11), 1462–1469.

SLICHTER, C. S. (1899). *Theoretical Investigations of the Motion of Ground Waters.* USGS, 19th Annual Report, Part II, 295–384.

SOARES-FRAZÃO, S. and V. GUINOT (2008). *A second-order semi-implicit hybrid scheme for one-dimensional Boussinesq-type waves in rectangular channels.* Int. J. Numer. Methods Fluids, 58(3), 237–261.

SOLLITT, C. K. and R. H. CROSS (1972). *Wave Reflection and Transmission at Permeable Breakwaters.* R. M. Parsons Laboratory Technical Report No. 147, MIT, Boston, MA, USA.

TISS, M. and R. D. EVANS (1989). *Measurement and correlation of non-Darcy flow coefficient in consolidated porous media.* J. Pet. Sci. Eng., 3(1-2), 19–33.

van GENT, M. R. A., H. A. H. PETIT and P. van den BOSCH (1994). *SKYLLA: Wave Motion in and on Coastal Structures - Implementation and Verification of Flow on and in Permeable Structures.* Delft Hydraulics Report H1780, Delft University of Technology, Delft, The Netherlands.

van GENT, M. R. A. (1995a). *Porous flow through rubble-mound material.* J. Waterw. Port Coast. Ocean Eng., 121(3), 176–181.

van GENT, M. R. A. (1995b). *Wave Interaction with Permeable Coastal Structures.* Ph.D. Thesis, Delft University of Technology, Delft, The Netherlands.

WHITAKER, S. (1996). *The Forchheimer equation: A theoretical development.* Transp. Porous Media, 25, 27–61.

WRIGHT, D. E. (1968). *Non-linear flow through granular media*. J. Hydraul. Div., 94(HY4), 851–872.

YAMAMOTO, S. and H. DAIGUJI (1993). *Higher-order accurate upwind schemes for solving the compressible Euler and Navier-Stokes equations.* Comput. Fluids, 22(2–3), 259–270.

ZERIHUN, Y. T. (2018). *Extension of the Dupuit–Forchheimer model for non-hydrostatic flows in unconfined aquifers*. Fluids, 3(2), doi:10.3390/fluids3020042.

ZERIHUN, Y. T. (2019). *On steady two-dimensional free-surface flows with spatially-varied discharges.* Slovak J. Civ. Eng., 27(3), 1–11.

ZERIHUN, Y. T. (2020a). *A numerical investigation of transient groundwater flows with a phreatic surface along complex hillslopes.* Slovak J. Civ. Eng., 28(1), 11–19.

ZERIHUN, Y. T. (2020b). *Free flow and discharge characteristics of trapezoidal-shaped weirs.* Fluids, 5(4), doi:10.3390/fluids5040238.

ZERIHUN, Y. T. (2023a). *Two-dimensional unconfined seepage flow toward a highway cut slope.* Acta Hydrotech., 36(65), 95–109.

ZERIHUN, Y. T. (2023b). *On the hydraulic characteristics of submerged flow over trapezoidal-shaped weirs.* Arch. Hydro-Eng. Environ. Mech., 70(1), 1–16.

ZERIHUN, Y. T. (2024). *Numerical modeling of sediment transport and bed evolution in nonuniform open-channel flows.* Arch. Hydro-Eng. Environ. Mech., 71(1), 1–26.